ATLAS NOTE

ATLAS-CONF-2014-062

November 22, 2014

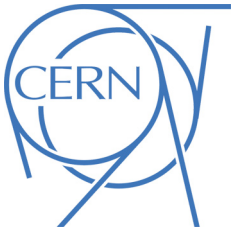

Search for Scalar-Charm Pair-Production with the ATLAS Detector in pp Collisions at $\sqrt{s} = 8$ TeV

The ATLAS Collaboration

Abstract

The results of a dedicated search for pair production of scalar partners of charm quarks are reported. The search is based on an integrated luminosity of 20.3 fb^{-1} of pp collisions at $\sqrt{s} = 8$ TeV recorded with the ATLAS detector. The search is performed using events with large missing transverse momentum and at least two jets, where the two leading jets are each tagged as originating from c quarks. Events containing isolated electrons or muons are vetoed. In an R-parity conserving minimal supersymmetric scenario in which a single scalar-charm state is kinematically accessible, and where it decays exclusively into a charm quark and a neutralino, 95% confidence-level upper limits are obtained in the $\tilde{c} - \tilde{\chi}_1^0$ mass plane such that, for neutralino masses below 200 GeV, scalar-charm masses up to 490 GeV are excluded.

ATLAS-CONF-2014-063
25 November 2014

Supersymmetry (SUSY) [1, 2, 3, 4, 5, 6, 7, 8, 9] is a theory that extends the Standard Model (SM) and naturally resolves the hierarchy problem by introducing supersymmetric partners of the known bosons and fermions. In the framework of a generic R-parity-conserving minimal supersymmetric extension of the SM, the MSSM [10, 11, 12, 13, 14], SUSY particles are produced in pairs and the lightest supersymmetric particle (LSP) is stable, providing a possible candidate for dark matter. In a large variety of models, the LSP is the lightest neutralino, $\tilde{\chi}_1^0$.

The scalar partners (squarks) of various flavours of quarks may, rather generally, have different masses despite constraints on quark flavour mixing [15]. Recent searches disfavour low-mass stops, sbottoms and gluinos, so direct scalar-charm ($\tilde{c}$) pair-production could be the only squark production process accessible at the LHC. Searches for $\tilde{c}$ states provide not only a possible supersymmetry discovery mode but also the potential to probe the flavour structure of the underlying theory.

Since no dedicated search for $\tilde{c}$ has been performed to date, the best existing lower limits on $\tilde{c}$ masses are obtained from searches for generic squark and gluino production at the LHC [16, 17], and from the reinterpretation of LHC searches [18] for direct pair production of the scalar partner of the top quark followed by decays $\tilde{t}_1 \to c + \tilde{\chi}_1^0$. The top squark searches have a similar final state to that expected for scalar charm quarks, but are optimized for small $m_{\tilde{t}} - m_{\tilde{\chi}_1^0}$ mass differences, so have good sensitivity to the scalar charm quark only when $m_{\tilde{c}} - m_{\tilde{\chi}_1^0} \lesssim m_W$.

In this note, a dedicated search for direct $\tilde{c}$ pair production is presented. The scalar charm is assumed to decay dominantly or exclusively via $\tilde{c} \to c + \tilde{\chi}_1^0$. The expected signal is therefore characterized by the presence of two jets originating from the hadronization of the c quarks, accompanied by missing transverse momentum ($E_{\mathrm{T}}^{\mathrm{miss}}$) resulting from the undetected neutralinos.

The ATLAS detector is described in detail elsewhere [19]. This search uses pp collision data at a center-of-mass energy of 8 TeV recorded during 2012 at the LHC. After the application of beam, detector and data quality requirements, the data set corresponds to a total integrated luminosity of 20.3 fb^{-1} with a 2.8% uncertainty, using the methods of Ref. [20].

The data are selected with a three-level trigger system that requires a high transverse momentum (p_{T}) jet and $E_{\mathrm{T}}^{\mathrm{miss}}$ [21]. While events containing charged leptons (electrons or muons) are vetoed in the search region, they are used in control regions, for which single-lepton triggers are used. Events are required to have a reconstructed primary vertex consistent with the beam positions, and to pass basic quality criteria which suppress detector noise and non-collision backgrounds [22]. Jets are reconstructed from three-dimensional topological calorimeter energy clusters by using the anti-k_t jet algorithm [23, 24] with a radius parameter of 0.4. The measured jet energy is corrected for inhomogeneities and for the non-compensating nature of the calorimeter by using p_{T}- and η-dependent[1] correction factors [25]. The impact of multiple overlapping pp interactions (pileup) is accounted for using a technique, based on jet areas, that provides an event-by-event and jet-by-jet correction [26]. Only jet candidates with $p_{\mathrm{T}} > 20\,\mathrm{GeV}$ within $|\eta| < 2.8$ are retained.

Electron candidates are required to have $p_{\mathrm{T}} > 7\,\mathrm{GeV}$, $|\eta| < 2.47$ and satisfy 'medium' selection criteria [27]. Muon candidates are required to have $p_{\mathrm{T}} > 6\,\mathrm{GeV}$, $|\eta| < 2.4$ and are identified as a match between an extrapolated inner-detector track and one or more track segments in the muon spectrometer [28]. When defining lepton (ℓ=e, μ) control regions, muons and electrons must pass additional 'tight' selection criteria [28, 29], and must satisfy track and calorimeter isolation criteria similar to those in Ref. [30].

Following this object reconstruction, overlaps between jet candidates and electrons or muons are resolved. Any jet within a distance $\Delta R = 0.2$ of a 'medium' quality electron candidate is discarded. Any remaining lepton within $\Delta R = 0.4$ of a jet is discarded. Remaining muons must have longitudinal and

[1] ATLAS uses a coordinate system with its origin at the nominal interaction point (IP) in the centre of the detector and the z-axis along the beam pipe. Cylindrical coordinates (r, ϕ) are used in the transverse plane, ϕ being the azimuthal angle around the beam pipe. The pseudorapidity is defined in terms of the polar angle θ as $\eta = -\ln\tan(\theta/2)$, while $\Delta R \equiv \left(\Delta\eta^2 + \Delta\phi^2\right)^{1/2}$.

transverse impact parameters within 1 mm and 0.2 mm of the primary vertex, respectively.

The calculation of $E_{\mathrm{T}}^{\mathrm{miss}}$ is based on the magnitude of the vector sum of the calibrated p_{T} of the reconstructed jets (with $p_{\mathrm{T}} > 20$ GeV and $|\eta| < 4.5$), electrons with $p_{\mathrm{T}} > 10$ GeV, muons with $p_{\mathrm{T}} > 6$ GeV and the calorimeter energy clusters not belonging to reconstructed objects [31].

Jets containing c-flavoured hadrons (without b-flavoured parent hadrons) are identified using a tagging algorithm based on a neural network that exploits both impact parameter and secondary vertex information. Jets can be c-tagged only within the acceptance of the inner detector ($|\eta| < 2.5$), so only such central jets are retained after the above selection. The efficiency for tagging b-jets is determined from measurements of dileptonic $t\bar{t}$ events [32]. The c-jet tagging efficiency and its uncertainty have been calibrated in inclusive jet events over a range of p_{T} using jets from collision data containing D^* mesons [33]. The parameters of the c-tagging algorithm are chosen such that a tagging efficiency of 19% (13%, 0.5%) is achieved for c-jets (b-jets, light flavour or gluon jets) in $t\bar{t}$ events.

Events are then required to have $E_{\mathrm{T}}^{\mathrm{miss}} > 150$ GeV and one jet with $p_{\mathrm{T}} > 130$ GeV to ensure full trigger efficiency, as well as a second jet with $p_{\mathrm{T}} > 100$ GeV. The two highest p_{T} jets are required to be c-tagged. The effect of pileup is mitigated by removing jets with $p_{\mathrm{T}} < 50$ GeV and within $|\eta| < 2.4$ if less than half of the p_{T} of the tracks associated with the jet is contributed by tracks matched to the primary vertex. The multijet background contribution with large $E_{\mathrm{T}}^{\mathrm{miss}}$, caused by mismeasurement of jet energies in the calorimeters or by neutrino production in heavy quark decays, is suppressed by requiring a minimum azimuthal separation ($\Delta\phi_{\mathrm{min}}$) between the $E_{\mathrm{T}}^{\mathrm{miss}}$ direction and any of the three leading jets of 0.4. In addition, the ratio of $E_{\mathrm{T}}^{\mathrm{miss}}$ to the transverse momenta of the two leading jets is required to be above one third. Events containing residual electron or muon candidates are vetoed in order to reduce electroweak backgrounds.

After these requirements, the main SM processes contributing to the background are top quark pair and single top production, together referred to as top production, as well as associated production of W/Z bosons with both light and heavy flavour jets, referred to as W+jets and Z+jets. A selection based on the boost-corrected contransverse mass m_{CT} [34] is employed to further discriminate scalar-charm pair from top production. For two identical decays of heavy particles into two visible particles v_1 and v_2, and into invisible particles, the contransverse mass [35] is defined as $([E_{\mathrm{T}}(v_1) + E_{\mathrm{T}}(v_2)]^2 - [\mathbf{p_T}(v_1) - \mathbf{p_T}(v_2)]^2)^{1/2}$. The boost-correction preserves the expected endpoint in the distribution against boosts caused by initial-state radiation. In the case of scalar-charm pair-production with $\tilde{c} \to c + \tilde{\chi}_1^0$, m_{CT} is expected to have an endpoint at $(m_{\tilde{c}}^2 - m_{\tilde{\chi}_1^0}^2)/m_{\tilde{c}}$. For $t\bar{t}$ production, if both b-jets are mis-tagged as c-jets, the m_{CT} built using those two jets is expected to have a kinematic endpoint at 135 GeV.

To maximize the sensitivity across the $\tilde{c}$–$\tilde{\chi}_1^0$ mass plane, three overlapping signal regions (SR) are defined requiring respectively $m_{\mathrm{CT}} > 150$, 200 and 250 GeV. The remaining $t\bar{t}$ background after the m_{CT} requirement comes mostly from events in which there is one true c-jet from a W decay and a mis-tagged b jet from a top quark decay. Events in which a Z boson is produced in association with heavy flavour jets where the Z boson decays into $\nu\bar{\nu}$ also enter the high-m_{CT} regions. The heavy flavour jets often originate from a gluon splitting $g \to c\bar{c}$, which can lead to small a angular separation between the resulting c-jets and therefore a small invariant mass m_{cc}. The remaining $t\bar{t}$ background is also concentrated at low m_{cc}. Consequently, a final requirement selects events for which the invariant mass of the two c-tagged jets is larger than 200 GeV.

Simulated-event samples are used to aid the description of the background and to model the SUSY signal. Top quark pair and single top production in the s- and Wt-channels are simulated with `POWHEG-1.0 (r2092)` [36], while the t-channel single top production is simulated using `ACERMC 3.8` [37]. A top quark mass of 172.5 GeV is used. The parton shower, fragmentation and hadronization are performed with `PYTHIA-6.426` [38]. Samples of W+jets, Z+jets and dibosons (WW, WZ, ZZ) with light and heavy flavour jets are generated with `SHERPA 1.4` [39], assuming massive b/c-quarks. Samples of $Zt\bar{t}$ and $Wt\bar{t}$ are generated with `MADGRAPH-5.1.3.33` [40] interfaced to `PYTHIA-6.426` [38]. The signal

samples are generated for a simplified SUSY model with only a single $\tilde{c}$ state kinematically accessible, and with BR($\tilde{c} \to c + \tilde{\chi}_1^0$)=100%, using MADGRAPH-5.1.5.11 interfaced to PYTHIA-6.427 for the parton shower, fragmentation and hadronization. Signal cross sections are calculated to next-to-leading order in the strong coupling constant, adding the resummation of soft gluon emission at next-to-leading-logarithmic accuracy (NLO+NLL) [41, 42, 43]. The nominal cross section and the uncertainty are taken from an envelope of cross section predictions using different PDF sets and factorisation and renormalisation scales, as described in Ref. [44]. The MC samples are processed through a detector simulation [45] based on GEANT4 [46]. The effects of pileup are included in the simulation. Efficiency corrections derived from the data are applied to the simulation to correct for lepton efficiency as well as the tagging and mis-tagging rates.

The main SM process contributing to the background after all signal region selections is Z+jets, followed by W+jets, top quark pair and single top production. The $t\bar{t}$ events contributing are semi-leptonic $t\bar{t}$ events, in which either the τ lepton decays hadronically, or the e or μ is out of the geometric acceptance or not reconstructed or identified. Contributions from multijet, diboson and associated production of $t\bar{t}$ with W, Z are sub-dominant. Non-collision backgrounds are found to be negligible.

The estimation of the main background processes is carried out by defining a set of three data control regions (CR) which have non-overlapping event selections amongst each other and with respect to the signal regions. The CRs are kinematically close to the SRs and each of them is enhanced in one of the backgrounds which is dominant in the SRs, while having low expected signal contamination. A statistical model is set up in which the background expectation in the CRs and SRs depends on several parameters of interest: the normalizations of the dominant backgrounds, top ($t\bar{t}$ + single top), Z+jets and W+jets, as well as on nuisance parameters including the effect of uncertainties on the jet energy scale (JES) and resolution, energy resolution of calorimeter clusters not associated with any physics objects, energy scale and resolution of electrons and muons, c- and mis-tagging rates, pileup and luminosity. A profile likelihood fit of the background expectation to the data is performed simultaneously in all CRs [47], and from it the background normalizations are extracted. The normalization factors, which are consistent with unity within uncertainties, are then applied to the MC expectation in the signal regions.

The first control region is populated largely by $t\bar{t}$ and W+jets. It contains events with exactly one isolated electron or muon with p_{T} above 50 GeV. The leading two jets must be c-tagged with $p_{\mathrm{T}} > 130$ GeV and 50 GeV. To select events containing $W \to \ell\nu$ the transverse mass of the $(\ell, E_{\mathrm{T}}^{\mathrm{miss}})$ system is required to be between 40 GeV and 100 GeV. The upper bound reduces possible signal contamination from any SUSY models which produce leptons in cascade decays. Finally, it is required that $E_{\mathrm{T}}^{\mathrm{miss}} > 100$ GeV and $m_{\mathrm{CT}} > 150$ GeV. The second control region is populated by $Z \to \ell^+\ell^-$ events with two opposite-sign, same-flavour leptons, where the minimum p_{T} requirement is 70 GeV for the leading lepton and 7(6) GeV for the sub-leading electron (muon). The momenta of the leptons are added vectorially to the $E_{\mathrm{T}}^{\mathrm{miss}}$ to mimic the $Z \to \nu\bar{\nu}$ decay, and the modulus of the resulting two-vector is required to be larger than 100 GeV. The leading two jets are required to be c-tagged and their p_{T} must each be above 50 GeV. The invariant mass $m_{\ell\ell}$ of the two leptons is required to be between 75 GeV and 105 GeV (Z-mass interval). A third control region, populated almost exclusively by dileptonic $t\bar{t}$ events, contains events with two opposite-sign, different-flavour leptons, where the leading lepton has $p_{\mathrm{T}} > 25$ GeV and the sub-leading lepton p_{T} is above 7(6) GeV for electrons (muons). It is required that $E_{\mathrm{T}}^{\mathrm{miss}} > 50$ GeV and $m_{\ell\ell} > 50$ GeV. The leading two jets are required to be c-tagged and have $p_{\mathrm{T}} > 50$ GeV. In all CRs, events with additional lepton candidates beyond the required number of signal leptons are vetoed applying the same lepton requirements used to veto events in the SRs.

The sub-dominant background contributions from dibosons, $Zt\bar{t}$ and $Wt\bar{t}$ are estimated by MC simulation. Finally, the residual multijet background is estimated using a data-driven technique based on the smearing of jets in a low $E_{\mathrm{T}}^{\mathrm{miss}}$ data sample with jet response functions [48].

The experimental and theoretical uncertainties affecting the main backgrounds are correlated be-

tween control and signal regions, and the data observed in control regions constrain the uncertainties on the expected yields in the signal regions. The residual uncertainty due to the theoretical modeling of the top production background is about 7%. It is evaluated using additional MC samples generated with ACERMC, where initial and final state radiation parameters were varied, an alternative fragmentation model (HERWIG), an alternative generator (MC@NLO) and an alternative $t\bar{t}$ vs single top Wt-channel overlap removal scheme. After the fit, the residual uncertainties on the W+jets and Z+jets theoretical modeling account for less than 20% of the total uncertainty. The dominant contributions to the residual uncertainty on the total background are from c tagging (∼20%), normalization uncertainties related to limited event numbers in the CRs (10% – 20%), and JES (∼10%).

For the SUSY signal processes, theoretical uncertainties on the cross section due to the choice of renormalization and factorization scales and from PDFs are found to be between 14% and 16% for $\tilde{c}$ masses between 100 GeV and 550 GeV. Prior to the fit, the detector-related uncertainties with most impact on the signal event yields are those for c-tagging (typically 15% – 30%) and JES (typically 10% – 30%).

m_{CT} (GeV)	>150	>200	>250
Top	7.4 ± 2.7 (7.1)	3.9 ± 1.6 (3.7)	1.6 ± 0.7 (1.5)
Z+jets	14 ± 3 (13)	7.7 ± 1.7 (7.0)	4.3 ± 1.2 (3.9)
W+jets	7.2 ± 4.5 (7.4)	4.1 ± 2.6 (4.2)	1.9 ± 1.2 (1.9)
Multijets	0.3 ± 0.3	0.2 ± 0.2	0.05 ± 0.05
Others	0.5 ± 0.3	0.4 ± 0.3	0.4 ± 0.3
Total	30 ± 6	16 ± 3	8.2 ± 1.9
Data	**19**	**11**	**4**

Table 1: Expected and observed number of events for an integrated luminosity of 20.3 fb^{-1} at $\sqrt{s}$ = 8 TeV. Top, Z+jets and W+jets contributions are estimated using the fit described in the text. For comparison, the numbers obtained using MC simulations only are shown in parentheses. The row labelled as 'Others' reports sub-dominant electro-weak backgrounds estimated from MC. The total uncertainties are also reported.

Table 1 reports the observed number of events and the SM predictions for each SR. The data are found to be systematically below the SM background expectations, but generally in agreement taking into account the uncertainties. Figure 1 shows the measured m_{CT} and m_{cc} distributions in the $m_{\mathrm{CT}} > 150$ GeV region compared to the SM predictions. MC estimates are shown after the normalizations extracted from the profile likelihood fit are applied. For illustrative purposes, the distributions expected for the simplified model with $(\tilde{c}, \tilde{\chi}_1^0)$ masses of (400, 200) GeV and (550, 50) GeV are also shown.

Since no significant excesses are observed, the results are translated into 95% confidence-level (C.L.) upper limits on contributions from new physics using the $\mathrm{CL_s}$ prescription [49]. Figure 2 shows the observed and expected exclusion limits at 95% C.L. on the $\tilde{c}$–$\tilde{\chi}_1^0$ mass plane, assuming a single accessible $\tilde{c}$ particle with $\mathrm{BR}(\tilde{c} \to c + \tilde{\chi}_1^0) = 100\%$. The SR with the best expected sensitivity at each point in the plot is adopted as the nominal result. In the region where the c-tagged SR of Ref. [18] provides a stronger expected limit, i.e. for $m_{\tilde{c}} - m_{\tilde{\chi}_1^0} \lesssim m_W$, it is that limit which is used. The area excluded by the 'monojet' SR of Ref. [18] is shown separately as a light shaded area. Systematic uncertainties, other than in the $\tilde{c}$ pair-production cross section, are treated as nuisance parameters and correlated when appropriate. For the SUSY scenario considered, the upper limit at 95% C.L. on the scalar-charm mass obtained in

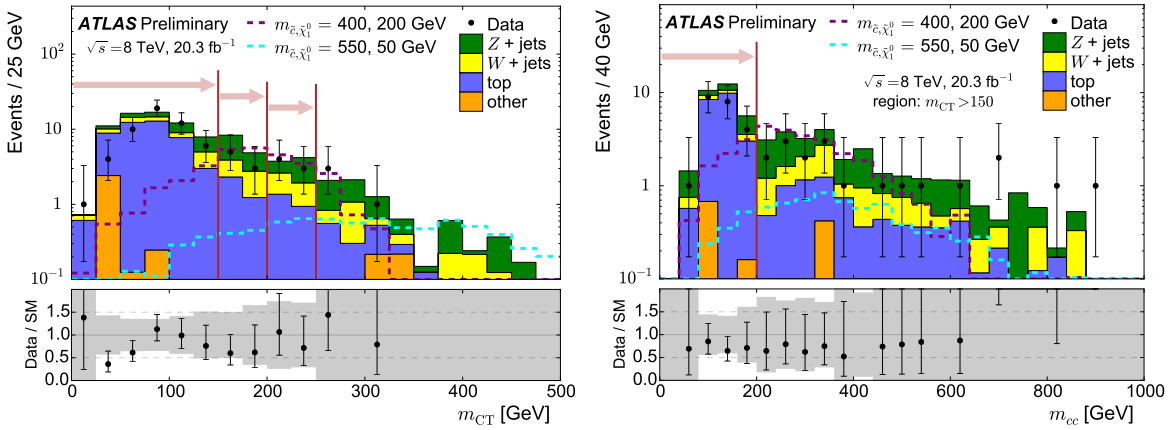

Figure 1: Distributions of m_{CT} (left) and m_{cc} (right), and their corresponding SM predictions. SR selections ($m_{\mathrm{CT}} > 150$ GeV for the m_{cc} distribution) are applied, other than for the variable plotted. Arrows indicate the SR requirements on m_{CT} and m_{cc}. In the ratio plots, the grey band corresponds to the combined MC statistical and experimental systematic uncertainty.

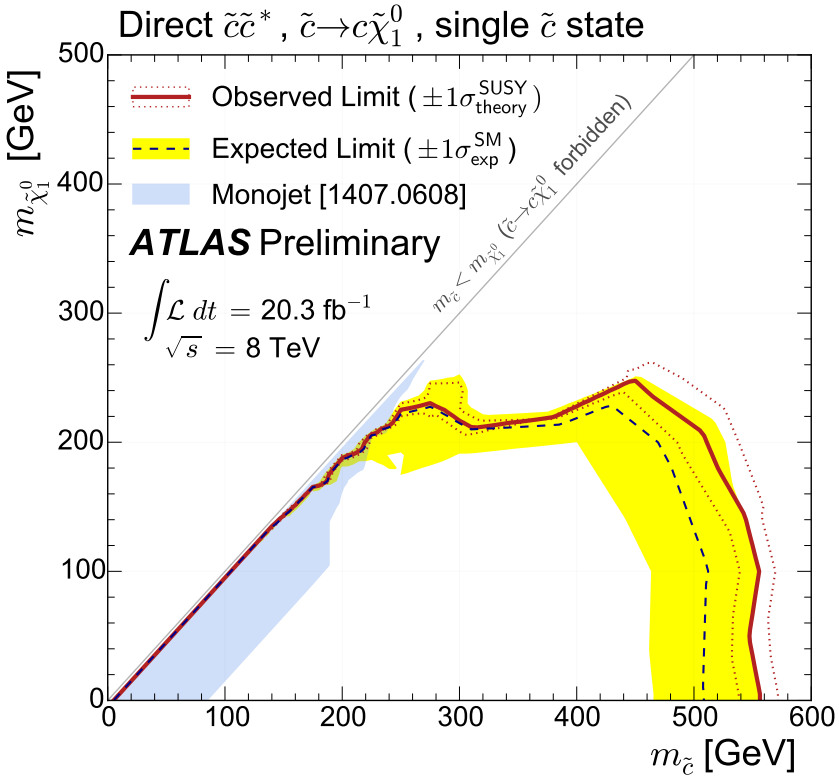

Figure 2: Exclusion limits at 95% C.L. in the $\tilde{c} - \tilde{\chi}_1^0$ mass plane (colour online). The observed (solid red line) and expected (dashed blue line) limits include all uncertainties except for the theoretical signal cross-section uncertainty (PDF and scale). The bands around the expected limits show $\pm 1\sigma$ uncertainties. The dotted lines around the observed limits represent the results obtained when moving the nominal signal cross section up or down by $\pm 1\sigma$ theoretical uncertainty.

the most conservative cross-section hypothesis is 540 GeV for $m_{\tilde{\chi}_1^0} = 0$ (increasing to 555 GeV for the central estimate of the signal cross section). Neutralino masses up to 200 GeV are similarly excluded for $m_{\tilde{c}} < 490$ GeV. This significantly extends the results of previous flavour-blind analyses [16, 17], which provide no exclusion for $m_{\tilde{\chi}_1^0} > 160$ GeV, nor for single light squarks with masses above 440 GeV. The signal regions are used to set limits on the effective cross section of new physics models, σ_{vis}, including the effects of branching ratios, experimental acceptance and efficiency, neglecting any possible contamination in the control regions. Values of σ_{vis} larger than 0.44 fb, 0.36 fb and 0.23 fb are excluded at 95% C.L. for m_{CT} greater than 150, 200 and 250 GeV respectively.

In summary, we report results of a search for scalar-charm pair-production in pp collisions at $\sqrt{s}$ = 8 TeV, based on 20.3 fb^{-1} of ATLAS data. The events are selected with large $E_{\text{T}}^{\text{miss}}$ and two c-tagged jets in the final state. The results are in agreement with SM predictions for backgrounds and translate into 95% C.L. upper limits on scalar-charm and neutralino masses in a simplified model with a single accessible $\tilde{c}$ state for which the exclusive decay $\tilde{c} \to c + \tilde{\chi}_1^0$ is assumed. For neutralino masses below 200 GeV, scalar-charm masses up to 490 GeV are excluded, significantly extending previous results.

References

[1] H. Miyazawa, Prog. Theor. Phys. **36** no. 6, (1966) 1266–1276.

[2] P. Ramond, Phys. Rev. **D3** (1971) 2415–2418.

[3] Y. Golfand and E. Likhtman, JETP Lett. **13** (1971) 323–326.

[4] A. Neveu and J. H. Schwarz, Nucl. Phys. **B31** (1971) 86–112.

[5] A. Neveu and J. H. Schwarz, Phys. Rev. **D4** (1971) 1109–1111.

[6] J. Gervais and B. Sakita, Nucl. Phys. **B34** (1971) 632–639.

[7] D. Volkov and V. Akulov, Phys. Lett. **B46** (1973) 109–110.

[8] J. Wess and B. Zumino, Phys. Lett. **B49** (1974) 52.

[9] J. Wess and B. Zumino, Nucl. Phys. **B70** (1974) 39–50.

[10] P. Fayet, Phys. Lett. **B64** (1976) 159.

[11] P. Fayet, Phys. Lett. **B69** (1977) 489.

[12] G. R. Farrar and P. Fayet, Phys. Lett. **B76** (1978) 575–579.

[13] P. Fayet, Phys. Lett. **B84** (1979) 416.

[14] S. Dimopoulos and H. Georgi, Nucl. Phys. **B193** (1981) 150.

[15] R. Mahbubani et al., Phys. Rev. Lett. **110** no. 15, (2013) 151804, arXiv:1212.3328 [hep-ph].

[16] ATLAS Collaboration, JHEP **09** (2014) 176, arXiv:1405.7875 [hep-ex].

[17] CMS Collaboration, JHEP **06** (2014) 055, arXiv:1402.4770 [hep-ex].

[18] ATLAS Collaboration, Phys. Rev. **D90** (2014) 052008, arXiv:1407.0608 [hep-ex].

[19] ATLAS Collaboration, JINST **3** (2008) S08003.

[20] ATLAS Collaboration, Eur. Phys. J. **C73** (2013) 2518, arXiv:1302.4393 [hep-ex].

[21] ATLAS Collaboration, Eur. Phys. J. **C72** (2012) 1849, arXiv:1110.1530 [hep-ex].

[22] ATLAS Collaboration, ATLAS-CONF-2012-020 (2012).

[23] M. Cacciari, G. P. Salam, and G. Soyez, JHEP **04**, 063 (2008), arXiv:0802.1189 [hep-ph].

[24] M. Cacciari and G. P. Salam, Phys. Lett. B **641** no. 1, (2006) 57 – 61, arXiv:hep-ph/0512210.

[25] ATLAS Collaboration, Eur. Phys. J. **C73** (2013) 2304, arXiv:1112.6426 [hep-ex].

[26] M. Cacciari and G. P. Salam, Phys. Lett. **B659** (2008) 119–126, arXiv:0707.1378 [hep-ph].

[27] ATLAS Collaboration, ATLAS-CONF-2014-032 (2014).

[28] ATLAS Collaboration, arXiv:1407.3935. Submitted to Eur. Phys. J. C.

[29] ATLAS Collaboration, Eur. Phys. J. **C72** (2012) 1909, arXiv:1110.3174 [hep-ex].

[30] ATLAS Collaboration, JHEP **10** (2013) 130, arXiv:1308.1841 [hep-ex].

[31] ATLAS Collaboration, ATLAS-CONF-2013-082, 2013.

[32] ATLAS Collaboration, ATLAS-CONF-2014-004, 2014.

[33] ATLAS Collaboration, ATLAS-CONF-2014-046, 2014.

[34] G. Polesello and D. Tovey, JHEP **03** (2010) 030, arXiv:0910.0174 [hep-ph].

[35] D. Tovey, JHEP **04** (2008) 034, arXiv:0802.2879 [hep-ph].

[36] S. Frixione et al., JHEP **11**, (2007) 070., arXiv:0709.2092 [hep-ph].

[37] B. P. Kersevan and E. Richter-Was, Comput. Phys. Commun. **184** (2013) 919–985, arXiv:0405247 [hep-ph].

[38] T. Sjöstrand, S. Mrenna, and P. Skands, JHEP **05**, 026 (2006) arXiv:0603175 [hep-ph].

[39] T. Gleisberg et al., JHEP **02** (2009) 007, arXiv:0811.4622 [hep-ph].

[40] J. Alwall et al., JHEP **06** (2011) 128, arXiv:1106.0522 [hep-ph].

[41] W. Beenakker et al., Nucl. Phys. **B515** (1998) 3–14, arXiv:hep-ph/9710451.

[42] W. Beenakker et al., JHEP **08** (2010) 098, arXiv:1006.4771 [hep-ph].

[43] W. Beenakker et al., Int. J. Mod. Phys. **A26** (2011) 2637–2664, arXiv:1105.1110 [hep-ph].

[44] M. Kramer et al., arXiv:1206.2892 [hep-ph].

[45] ATLAS Collaboration, Eur. Phys. J. **C70** (2010) 823–874, arXiv:1005.4568 [physics.ins-det].

[46] S. Agostinelli et al., Nucl. Instrum. Meth. **A506**, 250 (2003).

[47] M. Baak et al., arXiv:1410.1280 [hep-ex].

[48] ATLAS Collaboration, Phys. Rev. **D87** (2013) 012008, arXiv:1208.0949 [hep-ex].

[49] G. Cowan, K. Cranmer, E. Gross, and O. Vitells, Eur. Phys. J. **C71** (2011) 1554, arXiv:1007.1727 [physics.data-an].